Pseudogap and antiferromagnetic correlations in the Hubbard model

Alexandru Macridin[1], Mark Jarrell[1], Thomas Maier[2] and P. R. C. Kent[1,2]
[1] *University of Cincinnati, Cincinnati, Ohio, 45221, USA*
[2] *Oak Ridge National Laboratory, Oak Ridge, Tennessee, 37831, USA*
(Dated: September 7, 2005)

Using the dynamical cluster approximation we calculate the single-particle spectra of the Hubbard model with next-nearest neighbor hopping t' at small doping. We find that the pseudogap along the zone diagonal in the electron doped systems is due to long range antiferromagnetic correlations. The physics in the proximity of $(0, \pi)$ is dramatically influenced by t' and determined only by the short range correlations. The effect of t' on the low energy ARPES spectra is weak except close to the zone edge. The short range correlations are sufficient to yield a pseudogap in the magnetic susceptibility and produce shadow states which develop a gap with decreasing temperature.

arXiv:cond-mat/0509166 v1 7 Sep 2005

Introduction In contrast to conventional superconductors, the normal state of high T_c superconductors is not a Fermi liquid, and displays many properties which are not well understood. Elucidating the physics of the normal state is crucial for understanding the high T_c materials. The most unusual properties occur in the pseudogap region at low doping. It is characterized by strong antiferromagnetic (AF) correlations and a depletion of low energy states detected by both one and two-particle measurements [1]. However, unlike the d-wave superconducting phase which seems to be universal in all the cuprates [2, 3], the pseudogap region displays different properties in the electron and hole doped materials [4, 6]. In order to develop a theory for the high T_c superconductivity it is essential to have a better understanding of the asymmetry between the electron and the hole doped materials.

In the simple Hubbard model, or the closely related t-J model, the electron-hole asymmetry can be captured by including a finite next-nearest neighbor hopping t' [7, 8]. An appropriate t' strongly enhances AF correlations in electron doped systems and modifies the angle resolved photoemission spectra (ARPES). This behavior mirrors that of the cuprates. In the hole doped cuprates the antiferromagnetism is destroyed very quickly upon doping (persisting to only $\approx 2\%$ doping) [9] and the ARPES show well defined quasiparticles close to $(\pi/2, \pi/2)$ in the Brillouin zone (BZ) and gap states in the proximity of $(0, \pi)$ [4, 5, 10]. In the electron doped cuprates antiferromagnetism is much more robust (persisting to $\approx 15\%$ doping) [11] and the ARPES at small doping ($\approx 5\%$) shows sharp quasiparticles at the zone edge and gap states elsewhere in the BZ [6, 10]. In this Letter we employ a reliable technique, the dynamical cluster approximation (DCA) [12, 13] on relatively large clusters, to investigate the pseudogap and the single-particle spectra of the t-t'-U Hubbard model at small doping, addressing the role of the antiferromagnetic correlations in the pseudogap physics.

We find that in hole doped systems, the pseudogap emerges in the proximity of $(0, \pi)$, requires only short range correlations, and its magnitude and symmetry is strongly influenced by t'. In electron doped systems, the pseudogap emerges along the diagonal direction, as a direct consequence of AF scattering and requires long range AF correlations but not necessarily long range order. The hopping t' enhances the AF correlations in the electron doped system and produces this AF gap. We also find that the short range correlations are sufficient to yield a pseudogap signal in the magnetic susceptibility and produce shadow states which develop a gap with decreasing temperature.

Our conclusion about the nature of the pseudogap in the electron doped systems is different from that drawn from cluster perturbation theory (CPT) [14] calculations. For interaction U of the order of the bandwidth W, CPT finds that, even when only short range AF correlations are considered, the states along the diagonal direction develop a gap. This result persists even at larger doping, $\approx 15\%$, in disagreement with experiment where quasiparticles appear along the diagonal direction and gapped states remain only at the intersection of the AF zone boundary with the non-interacting Fermi surfaces (hot spots) [15]. In order to circumvent this the authors of Ref. [14] introduced two different mechanisms for the pseudogap in electron doped systems: a strong-coupling ($U \approx W$) pseudogap at small doping produced by short range correlations and a weak-coupling ($U < W$) pseudogap valid at intermediate doping which requires long range AF correlations. In contrast to the CPT results, we find no pseudogap along the diagonal direction for the strong coupling regime ($U = W$) unless long range AF correlations are considered, in better agreement with small coupling results in Ref. [14, 16]. Our results imply that there is no need to introduce two different pseudogap mechanisms for the electron doped systems. We believe that a plausible reason for the discrepancy between DCA and CPT results is the overestimation of AF correlations in the latter approach due to finite size effects [17] characteristic to small clusters [18] and lack of self-consistency [19].

Formalism The Hubbard Hamiltonian is

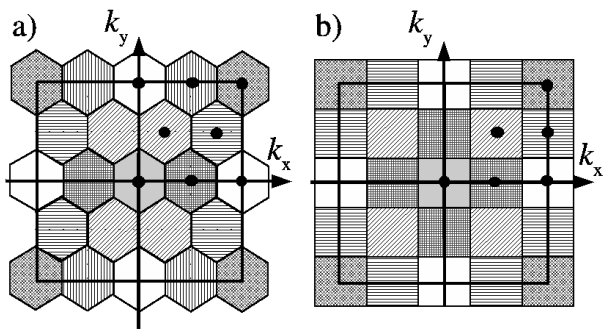

FIG. 1: For a 16 site cluster the BZ is coarse grained in 16 cells. a) and b) correspond to clusters with different geometry, 16A and respectively 16B as described in Ref. [21].

$$H = -t \sum_{\langle ij \rangle, \sigma} c^{\dagger}_{i\sigma} c_{j\sigma} - t' \sum_{\langle\langle il \rangle\rangle, \sigma} c^{\dagger}_{i\sigma} c_{l\sigma} + U \sum_{i} n_{i\uparrow} n_{i\downarrow} \ . \quad (1)$$

Here $c^{(\dagger)}_{i\sigma}$ destroys (creates) an electron with spin σ on site i and $n_{i\sigma}$ is the corresponding number operator. U is the on-site Coulomb repulsion. We consider hopping t between nearest-neighbors $\langle ij \rangle$ and hopping t' between next-nearest-neighbors $\langle\langle il \rangle\rangle$. In cuprates $t' \approx -0.3t$ [20] and hole (electron) doped systems correspond to a filling smaller (larger) than one. In our calculations, for ease of comparison between the electron and the hole doped cases, we keep the filling $n = 0.95$ and modify the sign of t', i.e. make it positive (negative) in order to represent the electron (hole) doped cuprates.

In the DCA [12] we map the original lattice model onto a periodic cluster of size $N_c = L_c \times L_c$ embedded in a self-consistent host. The correlations up to a range $\xi \lesssim L_c$ are treated accurately, while the physics on longer length-scales is described at the mean-field level. The reduction to an effective cluster model is achieved by coarse graining the BZ into N_c cells (see Fig. 1) and approximating the self-energy as a constant within each cell, $\Sigma(\mathbf{k}, \omega) \approx \Sigma(\mathbf{K}, \omega)$, where $\mathbf{K}$ denotes the center of the cell which $\mathbf{k}$ belongs to.

We solve the cluster problem using quantum Monte Carlo (QMC) [17]. The Maximum Entropy method[22] is employed to calculate the real frequency cluster Green's function from which the self-energy is extracted. It is then interpolated using a smooth spline, and used to calculate the lattice spectrum $A(k, \omega)$. We use two different 16 site cluster geometries, 16A and 16B [21], which result in different coarse graining of the BZ (see Fig. 1). Calculations on larger clusters below the pseudogap temperature and at large coupling ($U = W$) are not currently possible due to the QMC sign problem. We find identical results (within the error bars) in all the common points of the coarse-grained Brillouin zones, which shows that these 16 site clusters capture the momentum dependence

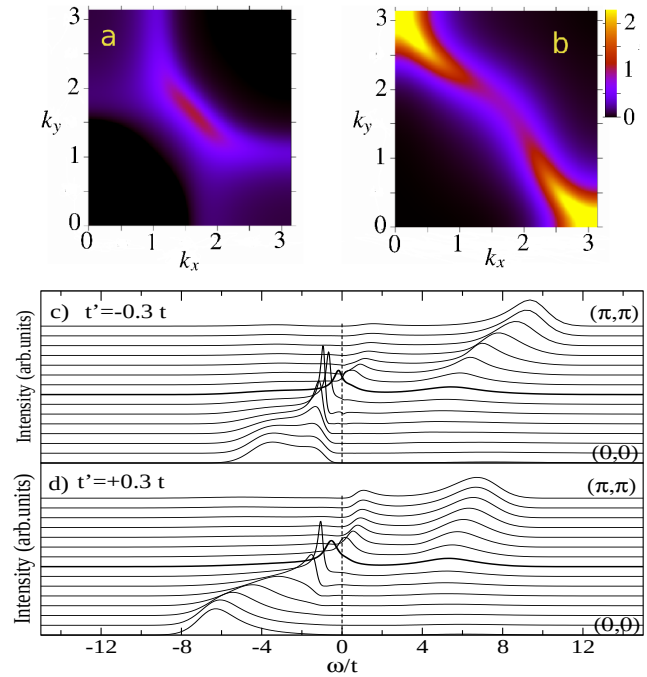

FIG. 2: (color) 5% doping. Zero energy surface $A(k, 0)$ for a) $t' = -0.3t$ and b) $t' = 0.3t$. $A(k, \omega)$ for k along the $(0,0)$-(π, π) direction in the BZ for c) $t' = -0.3t$ and d) $t' = 0.3t$.

of the self-energy rather well. We checked the robustness of our results at low temperature with calculations on smaller clusters where the sign problem is much better.

Results At a temperature $T_N = 0.19t$ ($0.24t$) for the hole (electron) doped system the AF correlation length reaches the cluster size yielding a divergent AF susceptibility (not shown). Below T_N one can proceed either by imposing the full symmetry on the effective medium, i.e. by reducing the problem to a cluster embedded in a paramagnetic (PM) host, or by allowing the host to develop long-range AF order. Both the PM and the AF solutions are complementary approximations to the exact solution; the first cuts off the AF correlations larger than the cluster size while the second one introduces long range AF order via the mean-field character of the host.

The *paramagnetic solution* will be discussed first. In Fig. 2 -a and -b we show the spectral intensity at zero energy for the hole and electron doped systems, respectively. These false color plots are very similar to the experimental ARPES data (see Fig.8 in Ref. [4] and Fig.3 in Ref. [6]). For instance, in both experiment and in our results, a region of large intensity can be observed close to $(\pi/2, \pi/2)$ and very low intensity is observed at the zone edge for hole doped systems. For the electron doped systems the intensity is maximum at $(0, \pi)$. However, the experimental data for the electron doped materials show gapped states along the diagonal direction [6]. Whereas, Fig. 2 -b reveals that in our calculations the intensity at $(\pi/2, \pi/2)$ is similar to the one observed

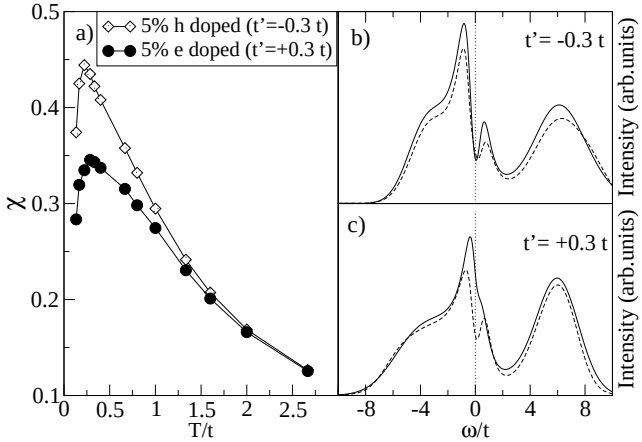

FIG. 3: a) Uniform ($k = 0$) spin susceptibility versus temperature for 5% hole (squares) and electron (circles) doped systems. Total DOS (full line) and DOS excluding the $(0, \pi)$ and $(\pi, 0)$ cells (dashed line) for hole doped (b) and electron doped (c) cases at $T = 0.12t$ and 5% doping.

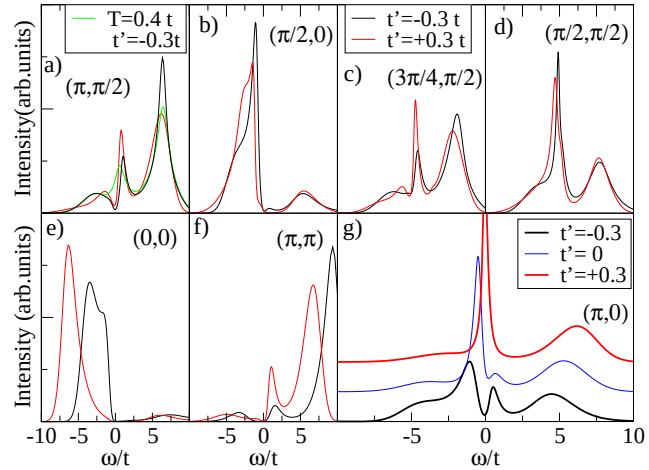

FIG. 4: (color) $A(k, \omega)$ for different k points in the BZ for hole (black) and electron (red) cases, at 5% doping and $T = 0.12t$. The green line in (a) is $A(k, \omega)$ for the hole doped case at larger $T = 0.4t$ which develops a gap upon decreasing T. In (g) the blue line represents the spectrum for $t' = 0$.

for the hole doped case and there is no pseudogap along the zone diagonal. In fact the cut of $A(k, \omega)$ along the diagonal direction shows very similar features for the hole and electron doped cases (Fig. 2-c and -d). Apart from the differences at high energy close to the zone center and the zone corner which follow the non-interacting dispersion, the low-energy features along the zone diagonal are almost identical.

In both experiment and our DCA calculations the pseudogap temperature T^* is associated with a downturn of the spin susceptibility with reduced temperatures [23]. We show the spin susceptibility versus temperature for 5% hole and electron doping in Fig. 3 -a. For both cases the downturn can be seen at $T = T^* \approx 2.4 \pm 0.1t$. For the hole doped case this T^* coincides roughly with the appearance of the pseudogap in the single particle spectra. However, for the electron doped case below the downturn temperature, no depletion in the total density of states at zero energy is seen (Fig. 3 -c, full line). The apparent reason for this lack of pseudogap in the total DOS of the electron doped systems is the large intensity peaks which emerge at the zone edge with decreasing temperature [24]. As shown in Fig. 3 -b and -c with the dashed lines, if one integrates the states in the BZ excluding those in the coarse-graining cell around $(0, \pi)$, a depletion of the low energy states with decreasing temperature can be noticed also for the electron doped case. Moreover, the resulting density of states is very similar to the one for the hole doped case.

A detailed comparison of the hole and electron spectra is presented in Fig. 4, where $A(K, \omega)$ for K in the center of the cells which divide the BZ [25] (see Fig. 1) are shown.

In Figs. 4 -a through -d, we find that the single particle spectra at low energy for the hole and the electron doped cases are surprisingly similar apart from the features close to $(0, \pi)$. The depletion of the low energy states shown in Fig 3 -b and -c with dashed lines, presumably associated with the downturn in the magnetic susceptibility, can be seen to come mostly from the states in the proximity of $(\pi, \pi/2)$ (see Fig. 4 -a). Unlike the non-interacting case, where at $(\pi, \pi/2)$, there is only spectral weight for $\omega > 0$, there is now substantial weight at negative energies. This is due to AF scattering as can be deduced by comparing the main features with the $(\pi/2, 0)$ spectrum (Fig. 4 -b) found at the mirroring position with respect to AF zone boundary in the BZ. These shadow states develop a gap with decreasing temperature as shown in Fig. 4 -a where a large temperature spectrum ($T = 0.4t$, green line) and a low temperature one ($T = 0.12t$, black line) are plotted for the hole doped case. In Fig. 4 -d we observe a sharp peak at $(\pi/2, \pi/2)$ in both the hole and electron doped spectra. Thus, there is no pseudogap along the diagonal direction.

Differences between the hole and electron doped spectra are illustrated in Figs. 4 -e through -g. In Figs. 4 -e and 4 -f one can see a difference between the hole and electron doped cases for the high energy features at zone center and respectively zone corner. This can be understood by noticing that t' shifts the the energy of these non-interacting states at these points by $4t'$. More significantly, a fundamental difference between the electron and hole doped spectra at $(0, \pi)$ is shown in Fig. 4-g. The hole doped spectra exhibits a strong gap whereas the electron doped spectra has an intense peak. It is also worth looking at the $t' = 0$ case, shown in the figure with dotted line, where a gap is present but it is much less developed than the one for $t' = -0.3t$. Thus, even for the hole doped case (i.e. $t' < 0$) the magnitude of t' has a strong

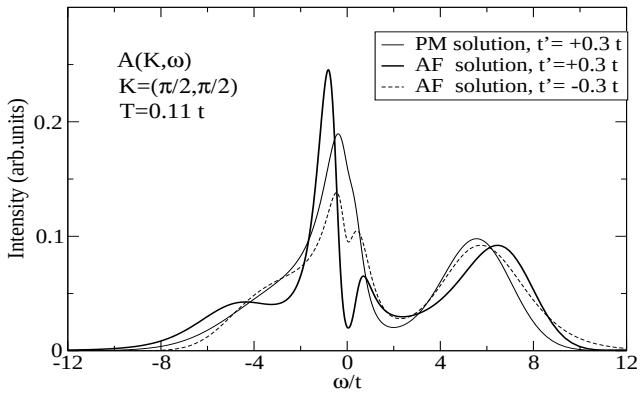

FIG. 5: $A(k,\omega)$ averaged over the $(\pi/2,\pi/2)$ cell for the AF and the PM solutions.

influence on symmetry with respect to zero energy of the density of states, which might be relevant for interpreting tunneling experiments. By comparing these results with earlier DCA calculations [8, 13] we also have found that the properties of $A(k,\omega)$ at $(0,\pi)$ can be rather successfully captured with a smaller 2×2 cluster, indicating that only the short range correlations of the order of one lattice spacing are relevant.

We will now discuss the *antiferromagnetic solution* (Fig. 5). Here, a gap is obtained for the electron doped case close to $(\pi/2,\pi/2)$ point in the BZ, in agreement with the experimental findings [6]. This gap is an antiferromagnetic (spin density wave) gap and requires long range AF correlations. The short range AF correlations, of the order of a few lattice constant, are not sufficient to produce it. This conclusion is in agreement with the small coupling pseudogap mechanism proposed in Ref. [14]. The hopping t' is responsible for enhancing the antiferromagnetism in the electron doped systems thus producing this gap. Presumably any other parameters which favor the antiferromagnetism will have a similar effect. For example, the AF solution for the hole doped case produces a gap at $(\pi/2,\pi/2)$ too, though a little smaller due to weaker antiferromagnetism. The spectral features away from $(\pi/2,\pi/2)$ within the AF solutions are not qualitatively different from the ones obtained with the PM solution (not shown). We note that the long range AF order does not yield a gap at $(0,\pi)$ for the electron doped case even though this point is on the AF zone boundary. The gap which the shadow states at $(\pi,\pi/2)$ develop in the PM solution is now enhanced by AF order, as well the intensity of the shadow states.

Band structure calculations suggest that a next-next-nearest-neighbor hopping $t''\approx 0.2t$ [20] should be included. We find that this term has a rather small quantitative effect (though it may provide better agreement with experimental data) and its presence would not change the conclusions of this investigation.

Conclusions Our calculation shows that the gap of the low-energy states along the diagonal direction of the BZ in the electron doped systems is an AF gap which requires long range AF correlations. On the other hand the physics in the proximity of $(0,\pi)$ is determined by the short range AF correlations and it is strongly influenced by t'. For the hole (electron) doped systems t' yields a gap (an intense peak) at the zone edge. Except in the proximity of the $(0,\pi)$ point in the BZ the influence of t' on the ARPES spectra is very weak. The short range AF correlations give rise to shadow states. These states develop a gap with decreasing temperature which coincides with the downturn in the spin susceptibility observed in both the hole and the electron doped systems.

Acknowledgment We thank George Sawatzky for useful discussions, and Kyle Shen and Donghui Lu for sharing their ARPES data. This research was supported by NSF Grants DMR-0312680 and DMR-0113574, by CMSN grant DOE DE-FG02-04ER46129 and by NSF cooperative agreement SCI-9619020 through resources provided by the San Diego Supercomputer Center.

[1] T. Timusk and B. Statt, Rep. Prog. Phys. **62**, 61, (1999); M.R. Norman *et. al*, Rep. Prog. Phys. **66**, 1547, (2003)
[2] C. C. Tsuei *et. al*, Phys. Rev. Lett.**73**, 593, (1994)
[3] C. C. Tsuei *et. al*, Phys. Rev. Lett.**85**, 182, (2000)
[4] F. Ronning *et. al*, Phys. Rev. B **67**, 165101, (2003)
[5] B.O. Wells *et al.*, Phys. Rev. Lett. **74**, 964 (1995)
[6] N. P. Armitage *et. al*, Phys. Rev. Lett.**88**, 257001, (2002).
[7] T. Tohyama and S. Maekawa, Phys. Rev. B **49**, 3596 (1993), Supercond. Sci. Technol. **13**, R17, (2000); R. J. Gooding *et al.* Phys. Rev. B **50**, 12866, (1994);
[8] A. Macridin *et al.* Phys. Rev. B **71**, 134527, (2005).
[9] Y. Kitaoka *et al.*, J. Phys. Soc. Jpn. **56**, 3024 (1987).
[10] A. Damascelli *et al.*, Rev. Mod. Phys. **75**, 473 (2003).
[11] G. M. Luke *et al.*, Phys. Rev. B 42, 7981 (1990).
[12] M. H. Hettler *et al.* Phys. Rev. B **58**, R7475 (1998); M. H. Hettler *et al.* Phys. Rev. B **61**,12739 (2000);
[13] Th. Maier *et al.*, cond-mat/0404055, to appear in Rev. Mod. Phys.
[14] D. Senechal *et al.*, Phys. Rev. Lett. **92**, 126401, (2004).
[15] N. P. Armitage *et. al*, Phys. Rev. Lett.**87**, 147003, (2001).
[16] B. Kyung *et al.*, Phys. Rev. Lett. **93**, 147004, (2004).
[17] M. Jarrell *et al.*, Phys.Rev. **B 64**,195130 (2001).
[18] T. Tohyama, Phys.Rev. **B 70**, 174517 (2004).
[19] C. Gros and R. Valenti, Annalen der Phys. **3**, 469, (1994); D. Senechal *et al.*, Phys. Rev. Lett.**84**, 522,(2000)
[20] O. Andersen *et al.*, J. Phys. Chem. Solids **56**, 1573 (1995).
[21] D. Betts *et al.*, Can. J. Phys. **77**, 353 (1999).
[22] M. Jarrell *et al.*, Physics Reports **269** No.3, 133, (1996).
[23] W. W. Warren *et al.*, Phys. Rev. Lett. **62**, 1193 (1989); M. Takigawa *et al.*, Phys. Rev. B **43**, 247 (1991); H. Alloul *et al.*, Phys. Rev. Lett. **70**, 1171 (1993).
[24] We obtained the same conclusion from an 8 site cluster calculation where it was possible to reach $T=0.05t$ for $U=W$.

[25] The self-energy in these K points results directly from DCA+MEM calculation. The self-energy in other momentum points in the BZ is obtained by interpolation.